Acta Oceanol. Sin., 2017, Vol. 36, No. 7, P. 56–65
DOI: 10.1007/s13131-017-1084-1
http://www.hyxb.org.cn
E-mail: hyxbe@263.net

A backscattering model for a stratified seafloor

YU Shengqi[1], LIU Baohua[1, 3*], YU Kaiben[1], YANG Zhiguo[1], KAN Guangming[2, 3]

[1] National Deep Sea Center, State Oceanic Administration, Qingdao 266237, China

[2] Key Laboratory of Marine Sedimentology and Environmental Geology, The First Institute of Oceanography, Qingdao 266061, China

[3] Laboratory for Marine Geology, Qingdao National Laboratory for Marine Science and Technology, Qingdao 266237, China

Received 9 October 2016; accepted 16 December 2016

Abstract

In order to predict the bottom backscattering strength more accurately, the stratified structure of the seafloor is considered. The seafloor is viewed as an elastic half-space basement covered by a fluid sediment layer with finite thickness. On the basis of calculating acoustic field in the water, the sediment layer, and the basement, four kinds of scattering mechanisms are taken into account, including roughness scattering from the water-sediment interface, volume scattering from the sediment layer, roughness scattering from the sediment-basement interface, and volume scattering from the basement. Then a backscattering model for a stratified seafloor applying to low frequency (0.1–10 kHz) is established. The simulation results show that the roughness scattering from the sediment-basement interface and the volume scattering from the basement are more prominent at relative low frequency (below 1.0 kHz). While with the increase of the frequency, the contribution of them to total bottom scattering gradually becomes weak. And the results ultimately approach to the predictions of the high-frequency (10–100 kHz) bottom scattering model. When the sound speed and attenuation of the shear wave in the basement gradually decrease, the prediction of the model tends to that of the full fluid model, which validates the backscattering model for the stratified seafloor in another aspect.

Key words: bottom backscattering model, stratified seafloor, sediment, basement

Citation: Yu Shengqi, Liu Baohua, Yu Kaiben, Yang Zhiguo, Kan Guangming. 2017. A backscattering model for a stratified seafloor. Acta Oceanologica Sinica, 36(7): 56–65, doi: 10.1007/s13131-017-1084-1

1 Introduction

Presently, the scattering model of Jackson et al. (1996) (Williams and Jackson, 1998) has been adopted extensively for the calculation of a bottom scattering strength at high frequency (10–100 kHz). In this mode, only the effect of surface layer of the sediment was taken into account. Bottom scattering was attributed to the seafloor roughness and the sediment heterogeneity, and the corresponding scattering strength was calculated by a composite-roughness scattering model and a volume scattering model considering refraction and attenuation in the sediment, respectively. The predicted bottom scattering strength agreed well with the measured data of several experimental sites with different sediment types.

Some more complex effects below the water-sediment interface, such as the sound speed gradient in the sediment and the seafloor stratification (Li et al., 1987), have been further considered in bottom scattering models since the 1990s, which are available to predict the bottom scattering strength at low frequency (100 Hz–10 kHz). In an early scattering model for an arbitrarily stratified seafloor (Ivakin, 1986), the effect of sediment volume scattering was merely taken into account. Specialized profiles of sound speed and density were employed to describe the continuous stratification. An analytic solution for acoustic field in the sediment was obtained, and the influence of internal boundaries on the frequency-angular dependence of the bottom scattering strength was demonstrated. In addition, the effect of continuous stratification was considered and some general properties of the backscattering strength were established by the WKB approximation. It was shown that the Lambert-like angular dependence could sometimes arise from the influence of a surface gradient on sediment volume scattering. In Efimov and Ivakin (1987), staircase functions were employed to approximately characterize arbitrary profiles, corresponding limitations in computation algorithms were discussed, and model-data comparisons were provided.

With the development of research, scattering caused by rough interfaces in layered sediments was further considered in bottom scattering models. In Ivakin (1994b), a first-order solution was presented for stratified fluid sediments with arbitrary number of interfaces, and the bottom bistatic scattering strength was expressed through the auto-spectra and cross-spectra of the roughness of different interfaces. In Ivakin (1994a), both roughness and volume scattering mechanisms were considered and compared. It was shown that the roughness and the volume scattering amplitudes for layered sediments can be denoted in a similar form. A somewhat different approach was presented in Essen (1994) and Moe and Jackson (1994), where the rough water-sediment interface was viewed as the only scattering mechanism, but the effect

Foundation item: The National Natural Science Foundation of China under contract Nos 41606081, 41330965 and 41527809; the Taishan Scholar Project Funding under contract No. tspd20161007.
*Corresponding author, E-mail: bhliu@ndsc.org.cn

of internal reflections due to stratification was contained. Some simplifications were introduced in Lyons et al. (1994), where the roughness and volume scattering in a two-layer system were processed. A treatment of the roughness scattering from a multilayered seafloor was demonstrated in Tang (1996), where the limit of close stacking of weakly scattering interfaces was shown to be indistinguishable from the volume scattering. In Ivakin (1998a), a unified perturbation approach to deal with the roughness and the volume scattering was presented, and generalized to the case that an arbitrary scattering basement was covered by stratified fluid sediment. The basement was assumed to be fluid (rough and/or heterogeneous) in numerical simulations of Efimov and Ivakin (1987) and Ivakin(1994b, 1998b), that is, the scattering from basement was considered, but ignored its elasticity. A numerical example of the scattering from a rough and heterogeneous elastic basement was presented in Ivakin (1997), which involved a first-order solution for the scattering amplitude of an elastic half-space medium (Ivakin, 1990; Ivakin and Jackson, 1998; Jackson and Ivakin, 1998). Finally, a geoacoustic bottom interaction model (GABIM) was established in Jackson et al. (2010), and corresponding calculation software was developed as well. Both roughness and volume scattering were considered in the GABIM, where the zeroth-order field solution required in the scattering kernels was calculated through the ocean acoustics and seismic exploration synthesis (OASES), and the volume scattering from the sediment with a complicated structure was expressed through an equivalent interface scattering cross section. The GABIM applies to the seafloor with arbitrary stratification, where the water-sediment interface is roughness, but allows only one internal roughness boundary (i.e., the sediment-basement interface). The sediment layers and the basement can all be heterogeneous responsible for the volume scattering, but the shear effect of the basement is only partly taken into account.

A simple and practical seafloor model is adopted in this paper. The seafloor is assumed to be made up of a fluid sediment layer with a finite thickness and an elastic half-space basement, and the shear effect of the basement is completely considered. On the basis of the seafloor model, a backscattering model for the stratified seafloor is established. The predicted bottom backscattering strength includes contributions of four kinds of scattering mechanisms, i.e., the roughness scattering from the water-sediment interface, the volume scattering from the sediment layer, the roughness scattering from the sediment-basement interface, and the volume scattering from the basement.

The paper is organized as follows. The stratified seafloor model and its parameterization are presented in Section 2. The acoustic filed solution in each layer is formulated as well. The backscattering model is established in Section 3. Section 4 demonstrates the simulation results, including the dependence of the backscattering strength on the acoustic frequency and the sediment-layer thickness, and the influence of shear effect of the basement on the backscattering strength. Finally, some conclusions are summarized in Section 5.

2 Seafloor model and parameterization

The bottom scattering model proposed in this paper applies to the prediction of the backscattering strength for stratified seafloors at low frequency. Because a transmission depth is relative deep in this frequency range, the influence of the seafloor stratification on the acoustic scattering becomes more significant. When a shallow bedrock exists in the seafloor, or the acoustic frequency is low enough that the sound wave interacts with the basement, a bottom scattering model based on the seafloor model shown in Fig. 1 is more reasonable. The seafloor is made up of a sediment layer with thickness of d and a half-space basement, and either layer possesses weak heterogeneity responsible for the volume scattering. Because there is a certain contrast of acoustic impedance between the unconsolidated sediment layer and the basement, the roughness scattering from the sediment-basement interface is further taken into account. Then the scattering mechanisms include the roughness scattering from the water-sediment interface, the volume scattering from the sediment layer, the roughness scattering from the sediment-basement interface, and the volume scattering from the basement.

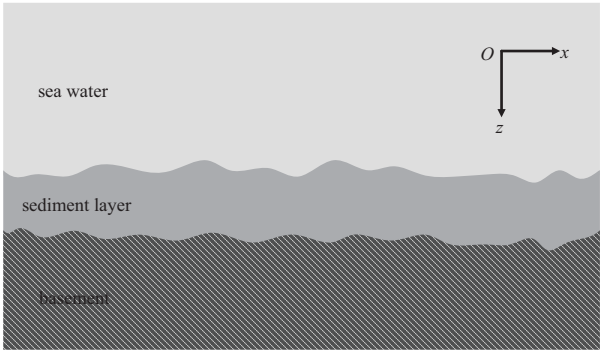

Fig. 1. Diagram of the seafloor model.

In the parameterization of the seafloor, the sediment layer is viewed as fluid, which is parameterized by compressional wave speed and attenuation and mass density. The basement is viewed as an elastic medium, whose shear effect is parameterized by shear wave speed and attenuation. It is further supposed that all the parameters are independent of depth in each layer with the exception of small random fluctuation responsible for the volume scattering. The speed and the density are expressed in the form of dimensionless ratios of corresponding parameters to that in the water as follows:

$$v_{\mathrm{p},n} = c_{\mathrm{p},n}/c_{\mathrm{w}}, \tag{1}$$

$$v_{\mathrm{t},2} = c_{\mathrm{t},2}/c_{\mathrm{w}}, \tag{2}$$

$$a_{\mathrm{p},n} = \rho_n/\rho_{\mathrm{w}}, \tag{3}$$

where the subscript n (=1, 2) represents the sediment layer and the basement, respectively; p denotes the compressional wave; t denotes the shear wave; c_{w} is the sound speed in the water (the acoustic absorption is ignored); ρ_n stands for the density of the sediment layer or the basement; and ρ_{w} is the density of the water. The attenuation of the sediment layer and the basement is given by loss parameters $\delta_{\mathrm{p},n}$ and $\delta_{\mathrm{t},2}$, which are related to the attenuation coefficient $\alpha_{\mathrm{p},n}$ and $\alpha_{\mathrm{t},2}$ in dB/m as

$$\alpha_{\mathrm{p},n} = \frac{40\pi f\,\delta_{\mathrm{p},n}}{v_{\mathrm{p},n}c_{\mathrm{w}}\ln 10}, \tag{4}$$

$$\alpha_{\mathrm{t},2} = \frac{40\pi f\,\delta_{\mathrm{t},2}}{v_{\mathrm{t},2}c_{\mathrm{w}}\ln 10}, \tag{5}$$

where f is the acoustic frequency.

The seafloor roughness is usually characterized by the rough-

ness spectrum in scattering models. One of the simplest and most often used isotropic spectral forms is the "power law":

$$W(\vec{K}) = \frac{w_2}{K^{\gamma_2}}, \tag{6}$$

where the parameter w_2 is called the spectral strength; and the parameter γ_2 is called the spectral exponent. Because the contribution of all scale roughness is considered in Eq. (6), this form of the roughness spectrum can be extended to low frequency in the case of being invariable of w_2 and γ_2.

The effect of acoustic refraction and transmission through the interface is considered in modeling of the volume scattering. The volume scattering is attributed to independent and isotropic point scatters in the sediment layer and the basement, and a dimensionless parameter is employed to quantify the volume scattering as follows:

$$\sigma_{2,n} = \frac{\sigma_{\mathrm{v},n}}{\alpha_{\mathrm{p},n}}, \tag{7}$$

where the commonly used approximation of single scattering is implied. The parameter $\sigma_{2,n}$ is referred to as the volume parameter; and the parameter $\sigma_{\mathrm{v},n}$ is the volume scattering cross section, which is assumed to be independent of depth in each layer. It is remarkable that besides the contribution of continuous heterogeneity to the volume scattering, possible discrete scatters or strong scattering layers are not considered in the volume scattering model.

When calculating the scattering strength of the stratified seafloor, it involves the pressure field in each layer derived from the incident plane wave in the water with unit strength. Because the seafloor model contains an elastic basement, it is more convenient to firstly solve the potential function of the displacement in stead of the pressure. According to the field theory, the displacement filed can be divided into

$$\vec{u}(\vec{r}) = \nabla\phi(\vec{r}) + \nabla\times\vec{\psi}(\vec{r}), \tag{8}$$

where ϕ is the scalar potential function of the displacement; and $\vec{\psi}$ is the vector potential function of the displacement. The former is used to describe the compressional wave, and the latter is for the shear wave. $\vec{r}$ is the position vector of an arbitrary space point. For a uniform medium, ϕ and $\vec{\psi}$ are subject to the following two uncoupled Helmholtz equations, respectively:

$$\nabla^2\phi + \frac{\omega^2}{c_{\mathrm{p}}^2}\phi = 0, \tag{9}$$

$$\nabla\times\nabla\times\vec{\psi} + \frac{\omega^2}{c_{\mathrm{t}}^2}\vec{\psi} = 0, \tag{10}$$

where c_{p} and c_{t} denote the compressional wave speed and the shear wave speed, respectively; and the parameter ω is the angular frequency.

It is supposed that the coordinate origin lies on the water-sediment interface and the positive direction is downwards. The formal solution of the scalar potential function of the displacement in the water can be written as

$$\phi_0(x,z,t) = A_0\mathrm{e}^{\mathrm{i}(k_{0,x}x - k_{0,z}z - \omega t)} + \mathrm{e}^{\mathrm{i}(k_{0,x}x + k_{0,z}z - \omega t)}, \tag{11}$$

where the coefficient A_0 indicates the complex amplitude of the reflected wave in the water.

The sediment is viewed as fluid, and the formal solution of the scalar potential function of the displacement in the sediment layer is

$$\phi_1(x,z,t) = A_1\mathrm{e}^{\mathrm{i}(k_{1,x}x - k_{1,z}z - \omega t)} + B_1\mathrm{e}^{\mathrm{i}(k_{1,x}x + k_{1,z}z - \omega t)}, \tag{12}$$

where the coefficients A_1 and B_1 indicate the complex amplitude of the up-going and down-going waves in the sediment layer, respectively.

The basement is viewed as an elastic medium, and the formal solution of the scalar and vector potential functions of the displacement (only with polarization of y direction) in the basement are

$$\phi_2(x,z,t) = B_2\mathrm{e}^{\mathrm{i}[k_{2,\mathrm{p},x}x + k_{2,\mathrm{p},z}(z-d) - \omega t]}, \tag{13}$$

$$\varphi_2(x,z,t) = C_2\mathrm{e}^{\mathrm{i}[k_{2,\mathrm{t},x}x + k_{2,\mathrm{t},z}(z-d) - \omega t]}, \tag{14}$$

where the coefficient B_2 indicates the complex amplitude of the down-going compressional wave in the basement; the coefficient C_2 indicates the complex amplitude of the down-going shear wave in the basement; $k_{0,z}$, $k_{1,z}$ and $k_{2,\mathrm{p},z}$ are the vertical components of wave vector of the compressional wave in each layer; $k_{2,\mathrm{t},z}$ is the vertical component of wave vector of the shear wave in the basement; and $k_{0,x}$, $k_{1,x}$, $k_{2,\mathrm{p},x}$ and $k_{2,\mathrm{t},x}$ are the corresponding horizontal component of the wave vector, respectively.

According to the continuity of the normal displacement and stress at the water-sediment boundary (z=0), one can obtain

$$\left.\frac{\partial\phi_0(x,z,t)}{\partial z}\right|_{z=0} = \left.\frac{\partial\phi_1(x,z,t)}{\partial z}\right|_{z=0}, \tag{15}$$

$$\left.\rho_0\frac{\partial^2\phi_0(x,z,t)}{\partial t^2}\right|_{z=0} = \left.\rho_1\frac{\partial^2\phi_1(x,z,t)}{\partial t^2}\right|_{z=0}. \tag{16}$$

According to continuity of the normal displacement and stress and zero of the shear stress at the sediment-basement boundary (z=d), one can obtain

$$\left.\frac{\partial\phi_1(x,z,t)}{\partial z}\right|_{z=d} = \left.\frac{\partial\phi_2(x,z,t)}{\partial z} + \frac{\partial\varphi_2(x,z,t)}{\partial x}\right|_{z=d}, \tag{17}$$

$$\left.\rho_1\frac{\partial^2\phi_1(x,z,t)}{\partial t^2}\right|_{z=d} = \rho_2\frac{\partial^2\phi_2(x,z,t)}{\partial t^2} + 2\rho_2c_{2,\mathrm{t}}^2\left\{\frac{\partial^2\varphi_2(x,z,t)}{\partial x\partial z} - \frac{\partial^2\phi_2(x,z,t)}{\partial x^2}\right\}\Bigg|_{z=d}, \tag{18}$$

$$\mu\left\{\frac{\partial^2\varphi_2(x,z,t)}{\partial x^2} - \frac{\partial^2\varphi_2(x,z,t)}{\partial z^2} + 2\frac{\partial^2\phi_2(x,z,t)}{\partial x\partial z}\right\}\Bigg|_{z=\mathrm{d}} = 0. \tag{19}$$

Substitute the corresponding formal solutions of scalar and vector potential functions of the displacement into above equations, one can obtain

$$k_{0,x} = k_{1,x} = k_{2,p,x} = k_{2,t,x} = k_x, \tag{20}$$

$$k_{0,z}A_0 - k_{1,z}A_1 + k_{1,z}B_1 = k_{0,z}\ , \tag{21}$$

$$\rho_0 A_0 - \rho_1 A_1 - \rho_1 B_1 = -\rho_0\ , \tag{22}$$

$$k_{1,z}\mathrm{e}^{-\mathrm{i}k_{1,z}d}A_1 - k_{1,z}\mathrm{e}^{\mathrm{i}k_{1,z}d}B_1 + k_{2,\mathrm{p},z}B_2 + k_{2,\mathrm{t},x}C_2 = 0, \tag{23}$$

$$\omega^2\rho_1\mathrm{e}^{-\mathrm{i}k_{1,z}d}A_1 + \omega^2\rho_1\mathrm{e}^{\mathrm{i}k_{1,z}d}B_1 + (2\rho_2 c_{2,\mathrm{t}}^2 k_{2,\mathrm{p},x}^2 - \omega^2\rho_2)B_2 - 2\rho_2 c_{2,\mathrm{t}}^2 k_{2,\mathrm{t},x}k_{2,\mathrm{t},z}C_2 = 0\ , \tag{24}$$

$$2k_{2,\mathrm{p},x}k_{2,\mathrm{p},z}B_2 + (k_{2,\mathrm{t},x}^2 - k_{2,\mathrm{t},z}^2)C_2 = 0. \tag{25}$$

Subsequently, coefficients A_0, A_1, B_0, B_2 and C_2 can be solved according to Eqs (21)–(25). The bottom reflection coefficient is

$$R_1(\theta) = A_0, \tag{26}$$

where the argument θ denotes the grazing angle of the incident wave in the water.

When calculating the roughness scattering from the water-sediment interface, the reflection coefficient $R_1(\theta)$ will be used. Coefficients A_1, B_1, B_2 and C_2 will be involved in the calculation of the volume scattering from the sediment layer and the basement. It is worth noting that these coefficients need to be multiplied by the density of corresponding layers to acquire the pressure.

3 Scattering model

When the seafloor model shown in Fig. 1 is adopted, the bottom scattering is sum of four kinds of mechanisms: the roughness scattering from the water-sediment interface, the volume scattering from the sediment layer, the roughness scattering from the sediment-basement interface, and the volume scattering from the basement. The bottom backscattering strength in dB is defined as

$$S_\mathrm{b}(\theta) = 10\lg[\sigma_\mathrm{sr}(\theta) + \sigma_\mathrm{sv}(\theta) + \sigma_\mathrm{br}(\theta) + \sigma_\mathrm{bv}(\theta)], \tag{27}$$

where σ_sr and σ_br denote the roughness scattering cross section of the water-sediment and sediment-basement interfaces, respectively; and σ_sv and σ_bv are the equivalent interface scattering cross section of the volume scattering from the sediment layer and the basement, respectively.

The stratification of the seafloor will also affect the bottom loss in dB, which is defined as

$$RL(\theta) = -20\lg[|R_1(\theta)|], \tag{28}$$

where $R_1(\theta)$ is the bottom reflection coefficient at the grazing angle θ.

3.1 *Roughness scattering*

Calculating the roughness scattering cross section of the water-sediment and sediment-basement interfaces is based on the composite-roughness scattering model of Jackson et al. (1996) (Williams and Jackson, 1998), where the reflection coefficient and the grazing angle need to be modified for the stratified seafloor. The roughness scattering cross section is a combination of the Kirchhoff and small-perturbation cross sections using the following interpolation scheme:

$$\sigma_\mathrm{r}(\theta) = [\sigma_\mathrm{kr}^\eta(\theta) + \sigma_\mathrm{pr}^\eta(\theta)]^{1/\eta}, \tag{29}$$

where the parameter η is usually assigned the value of –2; and σ_kr and σ_pr indicate the scattering cross section derived from the Kirchhoff and small-roughness perturbation approximations, respectively. The interpolation scheme obeys the rule of being dominant with the smaller one of the two approximations. Near the normal direction (corresponding to the specular reflection direction for bistatic case), it tends to Kirchhoff approximation. While for low grazing angles, it tends to the small-roughness perturbation approximation. So the accuracy of the predicted scattering strength can be balanced in the whole range of the grazing angle.

In Kirchhoff approximation, a rather difficult integral referred to as "Kirchhoff integral", needs calculating through a numerical method (Drumheller and Gragg, 2001). To avoid solving Kirchhoff integral for the more remarkable case of backscattering, the Kirchhoff cross section can be approximately by an algebraic fit (Mourad and Jackson, 1989) as follows:

$$\sigma_\mathrm{kr}(\theta) = \frac{bq_\mathrm{c}\,|R\,(90^\circ)|^2}{8\pi[\cos^{4\alpha}\theta + aq_\mathrm{c}^2\sin^4\theta]^{(1+\alpha)/2\alpha}}\ , \tag{30}$$

where R denotes the bottom reflection coefficient.

To guarantee that the roughness scattering cross section at small and middle grazing angles further favors the result of a small-roughness perturbation approximation, the Kirchhoff cross section should be multiplied by the following modified factor before using the interpolation scheme (Jackson et al., 2010):

$$F = 1 + 100\cos^4\theta\,. \tag{31}$$

This term is developed by a trial-and-error.

The scattering cross section derived from the small-roughness perturbation approximation can be expressed as

$$\sigma_\mathrm{pr} = k_0^4\,|A_\mathrm{ww}|^2\,W(\Delta\vec{K}), \tag{32}$$

where the coefficient A_ww is determined by the form of media to be based on, i.e., it has different expressions for fluid and elastic media; $W(\bullet)$ is the roughness spectrum; and $\Delta\vec{K}$ is the difference of horizontal parts of wave vector of the scattering wave and the incident wave, for backscattering, whose magnitude is

$$\Delta K = 2k_0\cos\theta. \tag{33}$$

In order to guarantee that the scattering cross section derived from the small-roughness perturbation approximation does not tend to be infinite near the normal incidence, the following value of ΔK is used as the argument of the roughness spectrum instead:

$$\Delta K = \sqrt{4k_0^2\cos^2\theta + (0.1k_0)^2}. \tag{34}$$

Although this treatment is somewhat arbitrary, the prediction of the composite-roughness scattering model (after the interpolation scheme) will be barely affected.

When calculating the backscattering strength of the stratified seafloor shown in Fig. 1, the reflection coefficient $R_1(\theta)$ is employed in the Kirchhoff and small-roughness perturbation approximations for the roughness scattering from the water-sediment interface.

For the roughness scattering from the sediment-basement in-

terface, calculations of the Kirchhoff and small-perturbation cross sections are based on the elastic theory (Jackson and Richardson, 2007). And the acoustic refraction is considered, where the grazing angle is substituted by

$$\theta_1 = \cos^{-1}(v_{\mathrm{p},1}\cos\theta). \tag{35}$$

The reflection coefficient adopts the value at the sediment-basement interface (the reflected wave is divided by the incident wave in the sediment layer, and take the ratio at z=d) as follows:

$$R_2(\theta_1) = \frac{A_1 \mathrm{e}^{-2\mathrm{i}k_{1,z}d}}{B_1}. \tag{36}$$

Subsequently, the roughness scattering cross section of the sediment-basement interface is reduced to the water-sediment interface, considering the energy loss of going in and out of the sediment layer. The result further needs to be multiplied by the following factor:

$$T(\theta) = |E\,\mathrm{e}^{\mathrm{i}k_{1,z}d}|^4 / a_{\rho,1}^2, \tag{37}$$

where E is the complex amplitude of the pressure of down-going wave in the sediment layer, which is related to the complex amplitude of the potential function of displacement by $E = a_{\rho,1}B_1$.

3.2 *Volume scattering*

To make the contribution of the volume scattering immediately add to that of the roughness scattering (i.e., satisfying Eq. (27)), the volume scattering from the sediment layer and basement needs to be viewed as a interface process and reduced to the water-sediment interface, leading to an equivalent interface scattering cross section. For getting the relationship between the equivalent interface scattering cross section σ_{v} and the volume scattering cross section σ_{vz}, another field variable (Ψ) is defined for convenience:

$$\Psi = \frac{p}{\sqrt{\rho}}, \tag{38}$$

where p is the pressure; and ρ is the density. For backscattering, the equivalent interface scattering cross section (Mourad and Jackson, 1993) can be expressed as

$$\sigma_{\mathrm{v}}(\theta) = \int_0^{\infty} |\Psi(z)|^4\, \sigma_{\mathrm{vz}}(z)\mathrm{d}z. \tag{39}$$

In each layer, σ_{vz} is supposed to be independent of depth, which can be obtained according to Eq. (7) and taken out of the integral under the condition that the volume heterogeneity is isotropic. Then the equivalent interface scattering cross section of the volume scattering from the sediment layer can be solved according to filed solutions (Jackson et al., 2010) as

$$\sigma_{\mathrm{sv}}(\theta) = \frac{\sigma_{\mathrm{v},1}}{a_{\rho,1}^2} \sum_{i1=1}^{2}\sum_{i2=1}^{2}\sum_{i3=1}^{2}\sum_{i4=1}^{2} a_{i1}a_{i2}^{*}a_{i3}a_{i4}^{*}F_{1,t}, \tag{40}$$

where

$$a_1 = A_1 a_{\rho,1}, \tag{41}$$

$$a_2 = B_1 a_{\rho,1}, \tag{42}$$

$$F_{1,t} = F_1[t(i1,i2,i3,i4)], \tag{43}$$

$$F_1(t) = \frac{\mathrm{e}^{td}-1}{t}, \tag{44}$$

$$t(i1,i2,i3,i4) = \mathrm{i}(g_{i1} - g_{i2}^{*} + g_{i3} - g_{i4}^{*}), \tag{45}$$

$$g_1 = -k_{1,z}, \tag{46}$$

$$g_2 = k_{1,z}. \tag{47}$$

There are down-going compressional and shear waves in the basement, so the equivalent interface scattering cross section of the volume scattering from the basement can be expressed by (referring to the volume scattering from the sediment layer)

$$\sigma_{\mathrm{bv}}(\theta) = \frac{\sigma_{\mathrm{v},2}}{a_{\rho,2}^2} \sum_{i1=1}^{2}\sum_{i2=1}^{2}\sum_{i3=1}^{2}\sum_{i4=1}^{2} a_{i1}a_{i2}^{*}a_{i3}a_{i4}^{*}F_{2,t}, \tag{48}$$

where

$$a_1 = a_{\rho,2}B_2, \tag{49}$$

$$a_2 = a_{\rho,2}C_2, \tag{50}$$

$$F_{2,t} = F_2[t(i1,i2,i3,i4)], \tag{51}$$

$$F_2(t) = -\frac{1}{t}, \tag{52}$$

$$g_1 = -k_{2,\mathrm{p},z}, \tag{53}$$

$$g_2 = -k_{2,\mathrm{t},z}. \tag{54}$$

4 Numerical simulations and discussion

For the stratified seafloor shown in Fig. 1, when the upper layer is a sandy sediment and the downer one is a rocky sediment, the parameters used for numerical simulations in this section are listed in Table 1. These parameters refer to Jackson and Ivakin (1998), Williams et al. (2002) and Jackson et al. (2010). The sound speed in the water is supposed to be 1 500 m/s.

4.1 *Influence of acoustic frequency and sediment-layer thickness on different scattering mechanisms*

The backscattering strength as a function of the grazing angle corresponding to different scattering mechanisms under the condition of several acoustic frequencies and sediment-layer thicknesses is shown in Fig. 2. In fact, the contribution of most discrete boundaries in the sediment to total bottom scattering is not large, which could be obvious and comparable with the volume scattering derived from the continuous heterogeneity in the case of more rough than the water-sediment interface and possessing relative large impedance contrast. Therefore, to highlight the contribution of the roughness scattering from the sediment-basement interface, the spectral strength is set to be a relative large value.

Table 1. Input parameters of the scattering model for the stratified seafloor

Parameter	Symbol	Unit	Value
Sound speed ratio of sandy sediment/water	$v_{\mathrm{p},1}$	dimensionless	1.1
Density ratio of sandy sediment/water	$a_{\rho,1}$	dimensionless	1.8
Loss parameter of sandy sediment	$\delta_{\mathrm{p},1}$	dimensionless	0.05
Spectral exponent of water-sediment interface	γ_{21}	dimensionless	3.25
Spectral strength of water-sediment interface	w_{21}	m^4	3.0×10^{-5}
Volume parameter of sandy sediment	σ_{21}	dimensionless	0.000 2
Ratio of compressional wave speed in basement to sound speed in water	$v_{\mathrm{p},2}$	dimensionless	2.1
Ratio of shear wave speed in basement to sound speed in water	$v_{\mathrm{t},2}$	dimensionless	1.5
Loss parameter of compressional wave in basement	$\delta_{\mathrm{p},2}$	dimensionless	0.02
Loss parameter of shear wave in basement	$\delta_{\mathrm{t},2}$	dimensionless	0.1
Density ratio of basement/water	$a_{\rho,2}$	dimensionless	2.5
Spectral exponent of sediment-basement interface	γ_{22}	dimensionless	3.25
Spectral strength of sediment-basement interface	w_{22}	m^4	0.005
Volume parameter of basement	σ_{22}	dimensionless	0.000 1

Comparing the simulation results under different conditions, it is found that the roughness scattering from the sediment-basement interface and volume scattering from the basement are more prominent at relative low frequency (below 1.0 kHz, as shown in Figs 2a and b). In particular, the roughness scattering strength of the sediment-basement interface may even exceed that of the water-sediment interface (besides the difference of interface roughness, another important reason is that the impedance contrast of sediment and basement is larger than that of water and sediment in simulations) Consequently, it is necessary to consider the contribution of the roughness scattering from the sediment-basement interface and the volume scattering from the basement at relative low frequency. Because the sound speed in the sandy sediment is larger than that of water, the total internal reflection will occur when the grazing angle is lower than the critical grazing angle (about 24.6° in this numerical example) of the sandy sediment (in this case, an evanescent wave exists in the sediment layer, which propagates horizontally but decays exponentially in the vertical direction) Thus there is an obvious transition in the curve of the roughness scattering strength of the sediment-basement interface near the critical grazing angle of the sandy sediment, which is the result of the difference of the roughness scattering from the sediment-basement interface caused by the evanescent wave and the normal propagation wave in the sediment layer. In addition, there is another transition near the critical grazing angle (about 61.6° in this numerical example) of the compressional wave in the basement for the same reason. As shown in Fig. 2a, the evanescent wave in the sediment layer produces more prominent volume scattering from the basement at relative low frequency. With the increase of frequency, the attenuation coefficient of the sediment layer gradually increases, while the attenuation of the evanescent wave is much larger than that of the normal propagation wave, which ultimately leads to a gradual decrease of the roughness scattering strength of the sediment-basement interface and the volume scattering strength of the basement, with a more significant decrease at subcritical grazing angles (in this case, their contributions to the total bottom scattering can even be ignored)

On the contrary, with the increase of frequency, the water-sediment interface becomes more "rough" compared with the length of sound wave. Then the roughness scattering strength of the water-sediment interface gradually increases. When the grazing angle is lower than the critical grazing angle of the sandy sediment, the volume scattering derived from the evanescent wave in the sediment layer is relative weak. With the increase of the grazing angle, the water-sediment interface becomes "transparent". And more acoustic energy transmits into the sediment layer, which leads to a gradual increase of the volume scattering strength of the sediment layer. It tends to be stable, when the sound wave goes through the whole sediment layer. With the increase of frequency, the attenuation coefficient of the sediment layer gradually increases, which leads to a somewhat decrease of the volume scattering strength of the sediment layer.

Comparing Fig. 2c with Fig. 2e, one can see that the influence of the acoustic frequency and the sediment-layer thickness on the backscattering strength is basically an inverse relationship. When the frequency decreases to a half and the thickness increases one times, the volume scattering strengths of the sediment layer and the basement are unchanged, while there is only a tiny variance of the roughness scattering strengths of the water-sediment and sediment-basement interfaces.

4.2 *Influence of acoustic frequency on bottom backscattering strength and bottom loss*

In order to analyze the influence of the acoustic frequency on the bottom backscattering strength and the bottom loss, the simulation results for a sediment layer with thickness of 2 m at different frequencies are presented in Fig. 3. Combining the analysis results of Fig. 2, it indicates that when the grazing angle is lower than the critical grazing angle of the sandy sediment, both roughness scattering from the sediment-basement interface and volume scattering from the basement are more prominent at relative low frequency (below 1.0 kHz). Subsequently, the total bottom scattering strength is relative large. However, with the increase of frequency, the contribution of them to the total bottom scattering enormously reduces, so that bottom backscattering strengths at different frequencies are almost the same. When the grazing angle is larger than the critical grazing angle of the sandy sediment, with the increase of frequency, only the roughness scattering from the water-sediment interface somewhat increases and the scattering strength derived from other scattering mechanisms performs various degrees of decreases, which leads to a result that the bottom scattering strength basically decreases with the increase of frequency. With the increase of frequency, the "trap" in the curve of the bottom backscattering strength near the critical grazing angle of the compressional wave in the basement gradually disappears. The whole curve becomes smoother and ultimately approaches to the prediction of the high-fre-

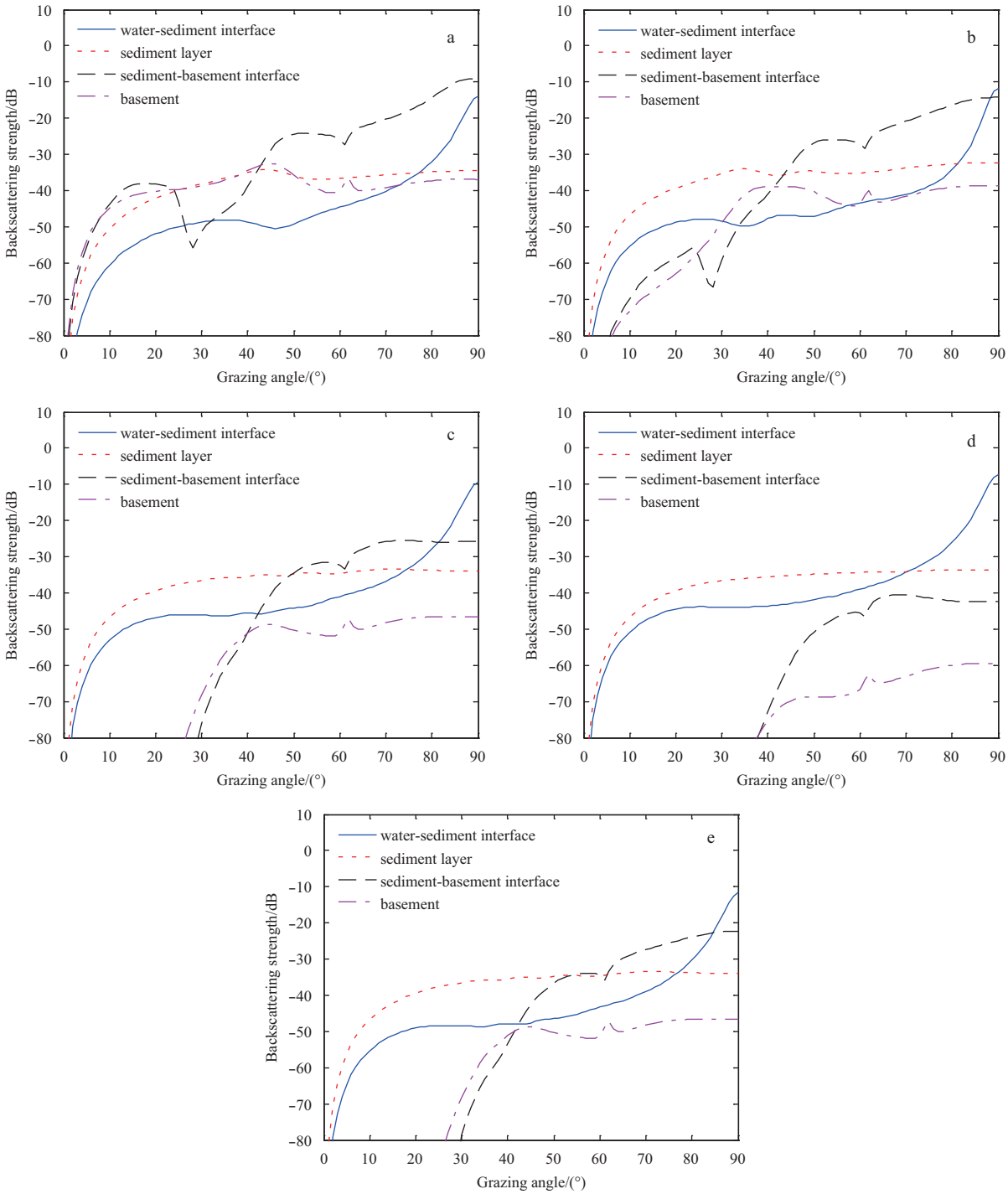

Fig. 2. The backscattering strength as a function of grazing angle corresponding to different scattering mechanisms. a. f=0.5 kHz and d=2 m, b. f=1.0 kHz and d=2 m, c. f=2.0 kHz and d=2 m, d. f=4.0 kHz and d=2 m, and e. f=1.0 kHz and d=4 m.

quency bottom scattering model of Jackson et al. (1996) (shown as the gray solid line in Fig. 3a, which only considers the effect of the surface layer of sediment. the seafloor is viewed as a half space of sediment) This result suggests that the contribution of the basement to the total bottom scattering can be neglected and the scattering model for the stratified seafloor degenerates to the high-frequency bottom scattering model at relative high frequency. At relative low frequency, bottom loss curves perform obvious vibration (except the case of 100 Hz, where the length of sound wave is much larger than the sediment-layer thickness and the effect of stratification is not evident) With the increase of frequency, both the vibration amplitude and period of bottom loss curves decrease, and the bottom loss gradually approaches to the reflection loss of water-sediment interface (shown as the gray solid line in Fig. 3b, which only considers the effect of the surface layer of sediment. The seafloor is viewed as a half space of sediment)

Subsequently, the bottom backscattering strength as a function of frequency at several grazing angles is presented in Fig. 4, where the sediment-layer thickness is 2 m. The simulation res-

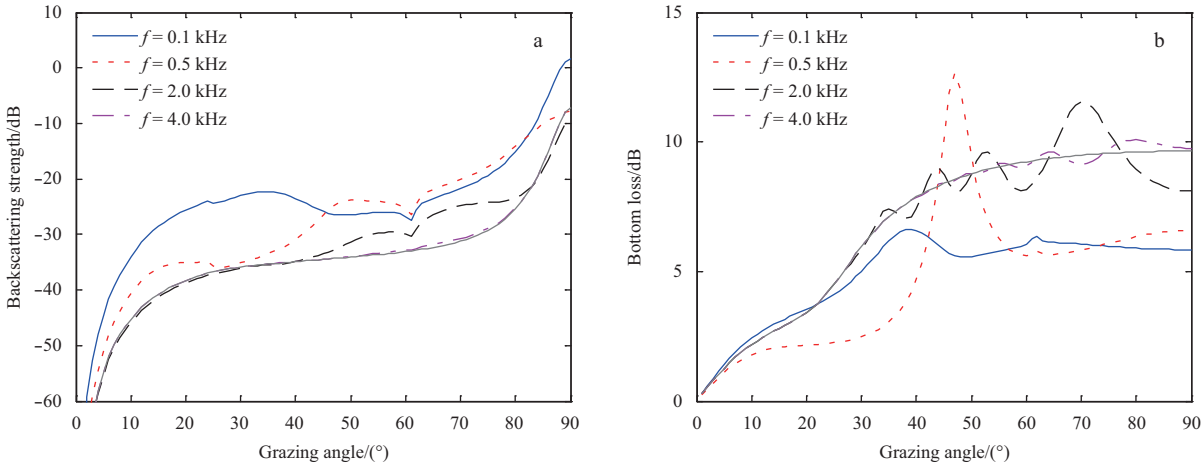

Fig. 3. The bottom backscattering strength and the bottom loss at different frequencies. The frequency is 4 kHz used in the high-frequency bottom scattering model. a. The backscattering strength, and b. the bottom loss.

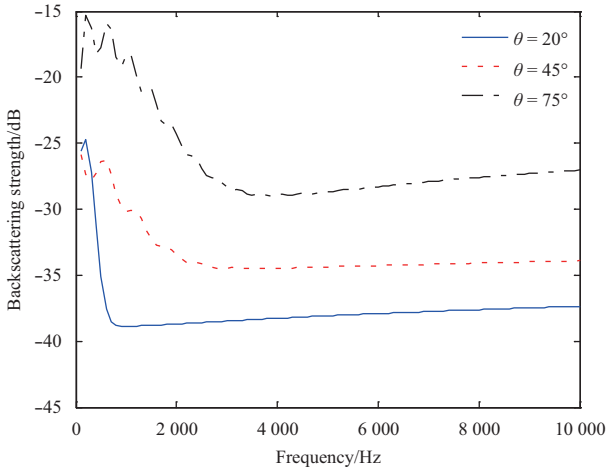

Fig. 4. The bottom backscattering strength as a function of frequency at several grazing angles.

ults show that the bottom backscattering strength as a function of frequency changes clearly and performs a certain vibration at relative low frequency. With the increase of the grazing angle, the bottom backscattering strength increases and its vibration amplitude and period decrease, while the frequency range with vibration becomes large. At relative high frequency, the bottom backscattering strength slowly increases with frequency, which approaches to the prediction of the high-frequency bottom scattering model of Jackson et al. (1996) as well.

4.3 *Influence of sediment-layer thickness on bottom backscattering strength and bottom loss*

In order to analyze the influence of the sediment-layer thickness on the bottom backscattering strength and the bottom loss, simulation results at 1 000 Hz for different thicknesses are presented in Fig. 5. The contribution of basement to the total bottom scattering declines with the increase of the sediment-layer thickness, where the variation regularity of the bottom backscattering strength is similar to that of the frequency dependence. While the influence of the thickness and the frequency on the bottom loss is completely complementary. When the frequency decreases to a half and the thickness increases one times, the bottom loss is unchanged. In other words, the bottom loss is a function of d/λ.

4.4 *Influence of shear effect of basement on bottom backscattering strength and bottom loss*

Finally, to analyze the influence of the shear effect of the basement on the bottom backscattering strength and the bottom loss, predictions for different shear wave speed and attenuation in the basement compared with that of a full fluid model (Jackson et al., 2010) (shown as the gray solid line, where the shear effect of the basemen is neglected) are presented in Fig. 6. In this case, the acoustic frequency is 1.0 kHz, the sediment-layer thickness is 2 m, and the sound speed in the water is assumed to be 1 500 m/s.

It is clearly found that the bottom backscattering strength and the bottom loss only perform contrast at middle grazing angles for different shear wave speed and attenuation. With the decrease of the shear wave speed and attenuation, the prediction considering the shear effect of the basement gradually approaches to that of the full fluid model, which can be viewed as a proof of the validity of the backscattering model for the stratified seafloor proposed in this paper.

5 Conclusions

A backscattering model for a stratified seafloor applying to low frequency (0.1–10 kHz) is established in this paper. In this model, the seafloor is viewed as an elastic half-space basement coved by a fluid sediment layer with a finite thickness. It is believed that the bottom scattering arises from four kinds of mechanisms, including the roughness scattering from the water-sediment interface, the volume scattering from the sediment layer, the roughness scattering from the sediment-basement interface, and the volume scattering from the basement. The numerical simulations of the influence of the acoustic frequency, the sediment-layer thickness, and the shear effect of the basement on the bottom backscattering strength as a function of the grazing angle are presented. The research shows that the roughness scattering from the sediment-basement interface and the volume scattering from the basement are more prominent at relative low frequency (below 1.0 kHz). The contribution of them to the total bottom scattering gradually becomes weak and declines faster at subcritical grazing angles with the increase of frequency. Then

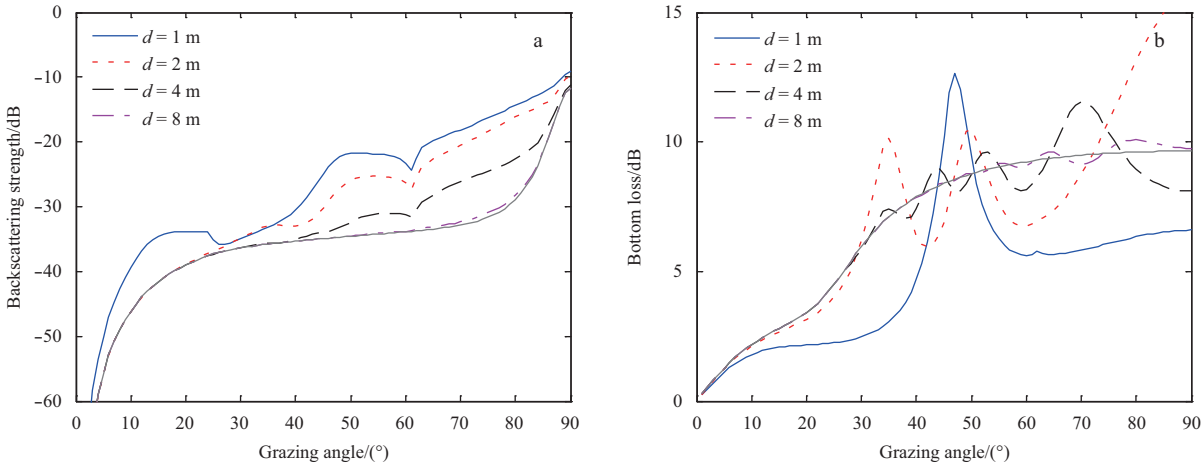

Fig. 5. The bottom backscattering strength and the bottom loss for different sediment-layer thicknesses. a. The backscattering strength and b. the bottom loss.

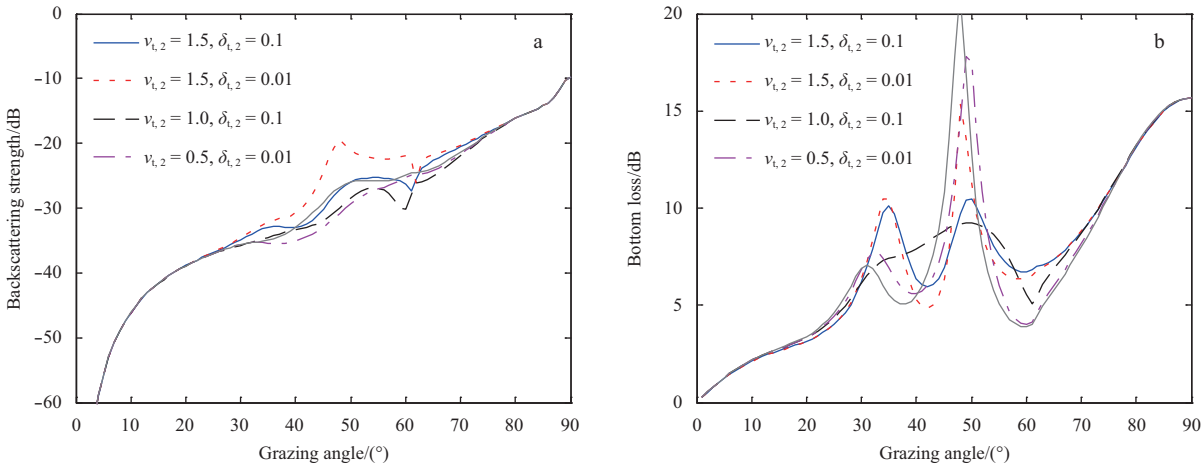

Fig. 6. The bottom backscattering strength and the bottom loss for different shear wave speed and attenuation. a. The backscattering strength and b. the bottom loss.

the prediction of the model ultimately approaches to that of the high-frequency bottom scattering model of Jackson et al. (1996). The variation regularity of the bottom backscattering strength with the increase of the sediment-layer thickness is similar to that of the frequency dependence. The backscattering strength as a function of the grazing angle gradually approaches to the prediction of the high-frequency bottom scattering model of Jackson et al. (1996) with the increase of the acoustic frequency or the sediment-layer thickness, which validates the backscattering model for the stratified seafloor in terms of the dependence of the acoustic frequency and the sediment-layer thickness. When the sound speed and attenuation of the shear wave in the basement gradually decreases, the prediction tends to that of the full fluid model, which provides another proof. Unfortunately, the model-data comparison is not presented in this paper, because some model parameters are hard or even impossible to measure in situ, such as the roughness under the sediment layer and the heterogeneity in the basement. At present, a try in a large water tank is in preparation. Measurements of the bottom backscattering strength and the model parameters will be synchronously carried out to validate the model through experiments in the near future.

References

Drumheller D M, Gragg R F. 2001. Evaluation of a fundamental integral in rough-surface scattering theory. The Journal of the Acoustical Society of America, 110(5): 2270–2275

Efimov A, Ivakin A. 1987. Sound scattering by inhomogeneities of layered sediments. Sudostroitelnaya Promyshlennost: Akustika (in Russian), 2(1): 24–31

Essen H H. 1994. Scattering from a rough sedimental seafloor containing shear and layering. The Journal of the Acoustical Society of America, 95(3): 1299–1310

Ivakin A N. 1986. Sound scattering by random inhomogeneities of stratified ocean sediments. Soviet Physics Acoustics, 32(6): 492–496

Ivakin A N. 1990. Sound scattering by inhomogeneities of an elastic half-space. Soviet Physics Acoustics, 36(4): 377–380

Ivakin A N. 1994a. Sound scattering by the rough interface and volume inhomogeneities of the sea bottom. Acoustical Physics, 40(3): 427–428

Ivakin A N. 1994b. Sound scattering by rough interfaces of layered media. In: Crocker M J, ed. Third International Congress on Air- and Structure-borne Sound and Vibration. Montreal, Canada: International Publications, 1563–1570

Ivakin A N. 1997. First-order model for bottom volume and roughness scattering. In: Zhang Renhe, Zhou Jixun, eds. Shallow-water Acoustics. Beijing: China Ocean Press, 359–364

Ivakin A N. 1998a. A unified approach to volume and roughness scattering. The Journal of the Acoustical Society of America, 103(2): 827–837

Ivakin A N. 1998b. Models for seafloor roughness and volume scattering. In: Jourdain J Y, ed. OCEANS'98 Conference Proceedings. Nice, France: OCEANS'98 IEEE/OES Conference Organizing Committee, 518–521

Ivakin A N, Jackson D R. 1998. Effects of shear elasticity on sea bed scattering: numerical examples. The Journal of the Acoustical Society of America, 103(1): 346–354

Jackson D R, Briggs K B, Williams K L, et al. 1996. Tests of models for high-frequency seafloor backscatter. IEEE Journal of Oceanic Engineering, 21(4): 458–470

Jackson D R, Ivakin A N. 1998. Scattering from elastic sea beds: first-order theory. The Journal of the Acoustical Society of America, 103(1): 336–345

Jackson D R, Odom R I, Boyd M L, et al. 2010. A geoacoustic bottom interaction model (GABIM). IEEE Journal of Oceanic Engineering, 35(3): 603–617

Jackson D R, Richardson M D. 2007. High-Frequency Seafloor Acoustics. New York: Springer Press, 338–348

Li Yuxin, Yang Yihua, Li Zhikuan, et al. 1987. An experimental study of deep scattering layer in the South China Sea. Acta Oceanologica Sinica, 6(1): 64–67

Lyons A P, Anderson A L, Dwan F S. 1994. Acoustic scattering from the seafloor: modeling and data comparison. The Journal of the Acoustical Society of America, 95(5): 2441–2451

Moe J E, Jackson D R. 1994. First-order perturbation solution for rough surface scattering cross section including the effects of gradients. The Journal of the Acoustical Society of America, 96(3): 1748–1754

Mourad P D, Jackson D R. 1989. High frequency sonar equation models for bottom backscatter and forward loss. In: Merry S L, ed. OCEANS'89 Conference Proceedings. Seattle, USA: OCEANS'98 IEEE/OES Conference Organizing Committee, 1168–1175

Mourad P D, Jackson D R. 1993. A model/data comparison for low-frequency bottom backscatter. The Journal of the Acoustical Society of America, 94(1): 344–358

Tang Dajun. 1996. A note on scattering by a stack of rough interfaces. The Journal of the Acoustical Society of America, 99(3): 1414–1418

Williams K L, Jackson D R. 1998. Bistatic bottom scattering: model, experiments, and model/data comparison. The Journal of the Acoustical Society of America, 103(1): 169–181

Williams K L, Jackson D R, Thorsos E I, et al. 2002. Acoustic backscattering experiments in a well characterized sand sediment: data/model comparisons using sediment fluid and Biot models. IEEE Journal of Oceanic Engineering, 27(3): 376–387